Electronic Supplementary Material (ESI) for RSC Advances.

Supporting Information

Synthesis, crystal structures, luminescent properties of Zn(II), Cd(II), Eu(III) complexes and detection of Fe(III) ions based on diacylhydrazone Schiff base.

Aiying Han, Hao Su, Guohong Xu, Maroof Ahmad Khan and Hui Li*

Key Laboratory of Cluster Science of Ministry of Education, School of Chemistry and Chemical Engineering, Beijing Institute of Technology, Beijing 100081, P. R. China

*E-mail: lihui@bit.edu.cn

Table of Content

^{1}H NMR, ^{13}C NMR spectra

IR Spectra

Crystal structures

Thermal stability

General spectroscopic methods

Optical properties

^{1}H NMR, ^{13}C NMR spectra

^{1}H NMR

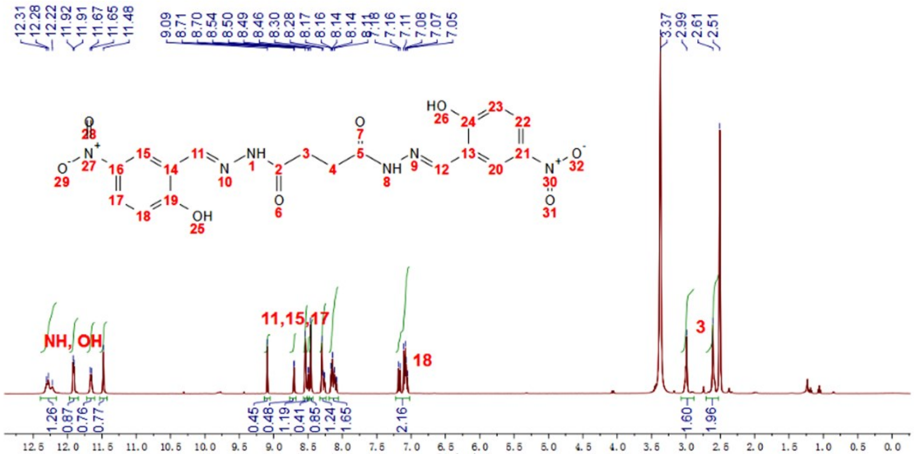

^{13}C NMR

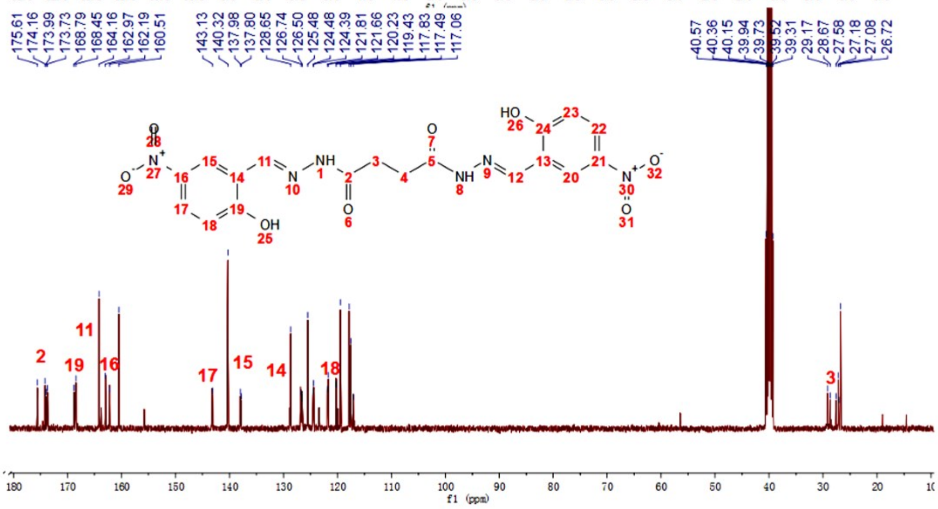

Fig. S1 ^{1}H NMR, ^{13}C NMR spectra of the ligand **H_4L** in DMSO-d^6 solution.

FT-IR analysis

FT-IR spectra of **H_4L** and complexes were shown in **Fig**. **2S**. When **H_4L** combined with metal ions, the characteristic absorption peaks obviously shifted. As for complex **Zn-L** and **Cd-L**, the peak of phenolic hydroxyl group at 3288 cm^{-1} shifted to 3430 cm^{-1} and 3441 cm^{-1}; the peak ascribed to carbonyl at 1647 cm^{-1} shifted to 1625 cm^{-1} and 1598cm^{-1}; the peak of imine carbon (C=N) at 1557 cm^{-1} shifted to 1552 and 1546cm^{-1} respectively. Similar to **Zn-L** and **Cd-L**, after binding to Eu^{3+}, the peaks of phenolic hydroxyl, carbonyl and imine group separately shifted to 3193 cm^{-1}, 1673 cm^{-1} and 1547 cm^{-1}. The above experimental results fully illustrated that Zn^{2+}, Cd^{2+} and Eu^{3+} bound with oxygen in phenolic hydroxyl group, oxygen in carbonyl group and nitrogen atoms in imine to form complexes.

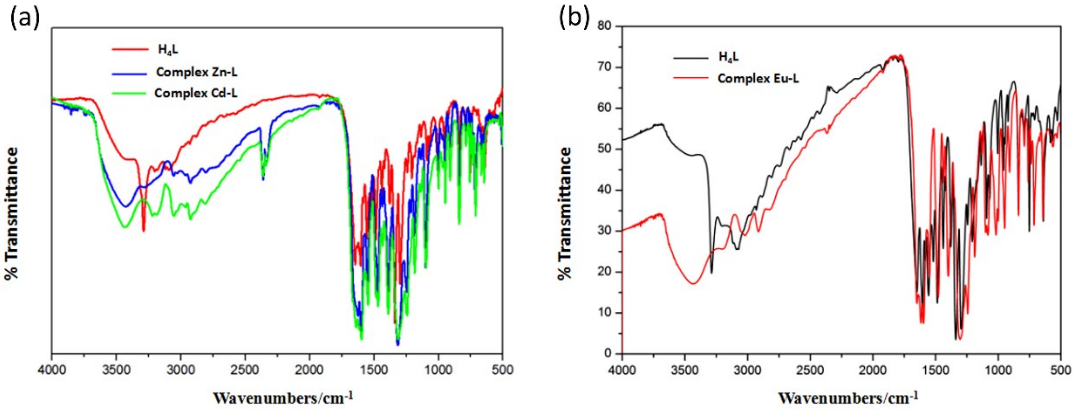

Fig. S2 FT-IR spectra of **H_4L** and complexes **Zn-L**, **Cd-L** (a) and **Eu-L** (b).

Crystal structures

Table S1 Lengths (Å) and angles (deg) of hydrogen bonds data for the complex **Zn-L**.

D—H···A	d(H···A)	d(D···A)	∠D—H···A
N2–H2···O9#1	1.869	2.697	160.93
N3–H3···O10#2	1.845	2.696	170.04

Symmetry transformations used to generate equivalent atoms: #1: -*x* + 2, -*y* + 2, -*z* + 1. #2: *x* + 1, *y*, *z*.

Table S2 Lengths (Å) and angles (deg) of hydrogen bonds data for the complex **Cd-L**.

D—H···A	d(H···A)	d(D···A)	∠D—H···A
N10–H10···O4#1	1.909	2.764	157.74
N3–H3···O16#2	2.049	2.808	141.31
N4–H4···O17#3	2.056	2.835	144.15
N9–H9···O18	2.013	2.791	143.83
O18–H18A···O17	1.975	2.824	177.94
O18–H18B···O10#4	1.963	2.813	177.32

Symmetry transformations used to generate equivalent atoms: #1: -*x* + 1, -*y* + 1, -*z*. #2: -*x* + 1, -*y* + 2, -*z* + 1. #3: *x* + 1, *y*, *z*. #4: -*x* + 1, -*y* + 1, -*z* + 1.

Table S3 Lengths (Å) and angles (deg) of hydrogen bonds data for the complex **Eu-L**.

D—H···A	d(H···A)	d(D···A)	∠D—H···A
N9—H9···O13	1.878	2.732	172.27
N4—H4···O15	1.892	2.749	174.40
N3—H3···O12#1	1.916	2.774	174.66
C30—H30C···O6#2	2.629	3.528	156.13
C29—H29B···O2#3	2.302	3.203	155.95

Symmetry transformations used to generate equivalent atoms: #1: -*x* + 1, -*y* + 1, -*z*+1. #2: x, -y, z-1/2. #3: x-1/2, y-1/2, -z+3/2.

Table S4 Selected bond distances (Å) and angles (deg) for the complexes **Zn-L**, **Cd-L** and **Eu-L**.

Complex **Zn-L**			
Zn1–O1	2.185(2)	N1–Zn1–O2#1	84.96(10)
Zn1–O4#1	2.017(2)	O3–Zn1–N1	87.08(11)
Zn1–O3	2.016(2)	O3–Zn1–O2#1	94.17(9)
Zn1–N4#1	2.088(3)	N4#1–Zn1–O1	92.22(10)
Zn1–N1	2.086(3)	N4#1–Zn1–O2#1	74.21(10)
Zn1–O2#1	2.242(2)	N1–Zn1–O1	75.58(10)
O4–Zn1#1	2.017(2)	N1–Zn1–N4#1	156.31(10)
N4–Zn1#1	2.088(3)	O1–Zn1–O2#1	87.90(9)
O2–Zn1#1	2.242(2)	N3–N4–Zn1#1	114.8(2)
O4#1–Zn1–O1	91.29(9)	C5–N1–Zn1	129.0(3)
O4#1–Zn1–N4#1	87.99(10)	N2–N1–Zn1	113.4(2)
O4#1–Zn1–N1	112.12(10)	C4–O2–Zn1#1	112.2(2)
O4#1–Zn1–O2#1	162.13(9)	C1–O1–Zn1	112.8(2)
O3–Zn1–O1	162.3(1)	C18–O4–Zn1#1	130.4(2)
O3–Zn1–O4#1	92.01(10)	C11–O3–Zn1	131.1(2)
O3–Zn1–N4#1	105.26(11)	C12–N4–Zn1#1	127.7(2)
Complex **Cd-L**			
Cd1–O11	2.189(3)	N10–N11–Cd2	114.01(18)
Cd1–O10	2.234(2)	C7–N2–Cd2	130.94(21)
Cd1–N5	2.304(3)	N3–N2–Cd2	112.31(18)
Cd1–O12	2.328(2)	C22–O3–Cd2	133.49(21)
Cd1–N8	2.334(3)	C8–O7–Cd2	115.45(21)
Cd1–O9	2.352(2)	C29–O9–Cd1	116.35(20)
Cd2–O3	2.214(2)	C26–O8–Cd2	115.39(20)
Cd2–O4	2.246(2)	C4–O4–Cd2	132.89(19)
Cd2–N11	2.302(3)	C11–O12–Cd1	115.41(20)
Cd2–N2	2.304(3)	C30–N8–Cd1	129.90(22)
Cd2–O7	2.327(3)	N9–N8–Cd1	113.82(18)
Cd2–O8	2.349(2)	C12–N5–Cd1	128.34(21)
O11–Cd1–O10	92.78(10)	N4–N5–Cd1	113.60(19)
O11–Cd1–N5	127.41(10)	C18–O10–Cd1	129.60(20)
O10–Cd1–N5	79.45(9)	C32–O11–Cd1	135.41(23)
O11–Cd1–O12	92.00(10)	C25–N11–Cd2	129.56(21)
O10–Cd1–O12	145.02(8)	O4–Cd2–N11	107.90(9)
N5–Cd1–O12	70.26(9)	O3–Cd2–N2	107.94(9)
O11–Cd1–N8	79.75(10)	O4–Cd2–N2	79.63(9)
O10–Cd1–N8	113.50(9)	N11–Cd2–N2	168.88(9)
N5–Cd1–N8	150.69(9)	O3–Cd2–O7	98.28(9)
O12–Cd1–N8	101.45(9)	O4–Cd2–O7	150.38(8)

O11–Cd1–O9	148.92(9)	N11–Cd2–O7	100.66(9)
O10–Cd1–O9	96.39(9)	N2–Cd2–O7	71.01(9)
N5–Cd1–O9	83.54(9)	O3–Cd2–O8	149.90(8)
O12–Cd1–O9	97.15(9)	O4–Cd2–O8	91.26(9)
O3–Cd2–N11	80.11(9)	N11–Cd2–O8	70.04(8)
O3–Cd2–O4	94.26(9)	N2–Cd2–O8	102.16(9)
Complex **Eu-L**			
Eu1–O3	2.313(5)	O4–Eu1–N8	64.24(17)
Eu1–O6#1	2.321(5)	O3–Eu1–N5#1	69.18(19)
Eu1–O008	2.325(5)	O6#1–Eu1–N5#1	67.57(17)
Eu1–O5#1	2.439(5)	O008–Eu1–N5#1	140.13(18)
Eu1–O11	2.463(5)	O5#1–Eu1–N5#1	62.13(16)
Eu1–O4	2.460(5)	O4–Eu1–O11	78.00(16)
Eu1–N8	2.599(6)	O11–Eu1–N5#1	72.03(18)
Eu1–N5#1	2.663(6)	O4–Eu1–N5#1	140.00(16)
Eu1–N2	2.676(6)	N8–Eu1–N5#1	120.78(18)
O3–Eu1–O6#1	86.52(19)	O3–Eu1–N2	67.62(18)
O3–Eu1–O008	85.37(18)	O6#1–Eu1–N2	148.49(19)
O6#1–Eu1–O008	81.17(20)	O008–Eu1–N2	79.16(18)
O3–Eu1–O5#1	80.55(17)	O5#1–Eu1–N2	65.66(17)
O6#1–Eu1–O5#1	129.46(17)	O11–Eu1–N2	122.49(17)
O008–Eu1–O5#1	144.81(18)	O4–Eu1–N2	61.00(17)
O3–Eu1–O11	139.36(17)	N8–Eu1–N2	120.48(18)
O6#1–Eu1–O11	88.82(18)	N51–Eu1–N2	115.36(17)
O008–Eu1–O11	133.31(16)	C8–O4–Eu1	125.48(4)
O5#1–Eu1–O11	71.87(16)	C11–O5–Eu1#1	124.67(4)
O3–Eu1–O4	128.27(17)	C26–O11–Eu1	121.04(4)
O6#1–Eu1–O4	138.22(17)	C23–O008–Eu1	141.90(5)
O008–Eu1–O4	79.86(17)	C25–N8–Eu1	132.10(5)
O5#1–Eu1–O4	83.89(15)	N9–N8–Eu1	112.32(4)
O3–Eu1–N8	150.59(18)	C14–O6–Eu1#1	141.64(5)
O6#1–Eu1–N8	74.35(18)	C12–N5–Eu1#1	131.19(5)
O008–Eu1–N8	69.99(17)	N4–N5–Eu1#1	112.68(4)
O5#1–Eu1–N8	128.85(17)	C7–N2–Eu1	131.11(5)
O11–Eu1–N8	63.40(17)	N3–N2-Eu1	113.58(4)

Symmetry transformations used to generate equivalent atoms: #1: *x*, 1.5 - *y*, 0.5 - *z*.

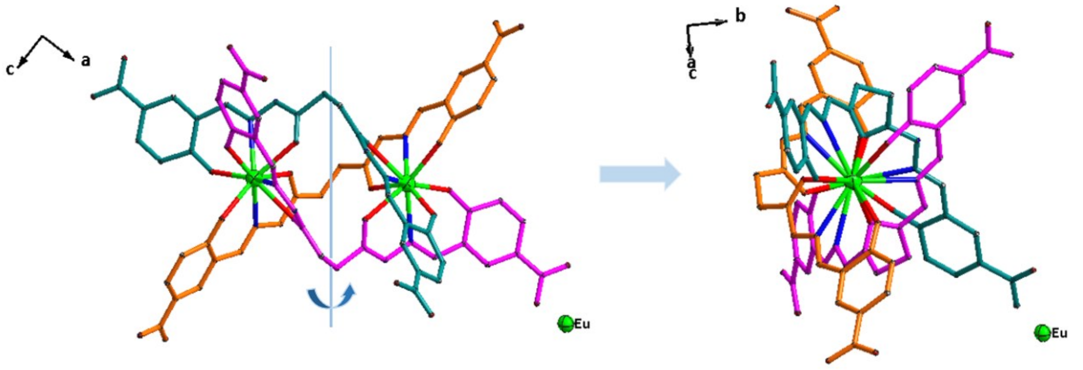

Fig. S3 Dinuclear structure of **Eu-L** coordinated with three ligands, when the rotation causes the two europium ions to coincide, the coordination bonds do not coincide completely, and the terminal ternate coronary structures are cross-aligned.

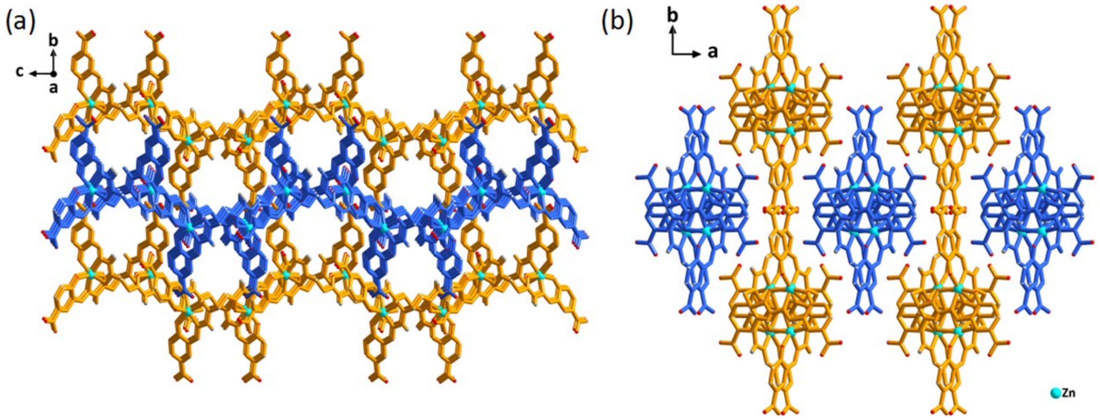

Fig. S4 3D supramolecular structure of Zn-L from a axis (a) and c axis (b). solvent molecules and anions are omitted for clarity.

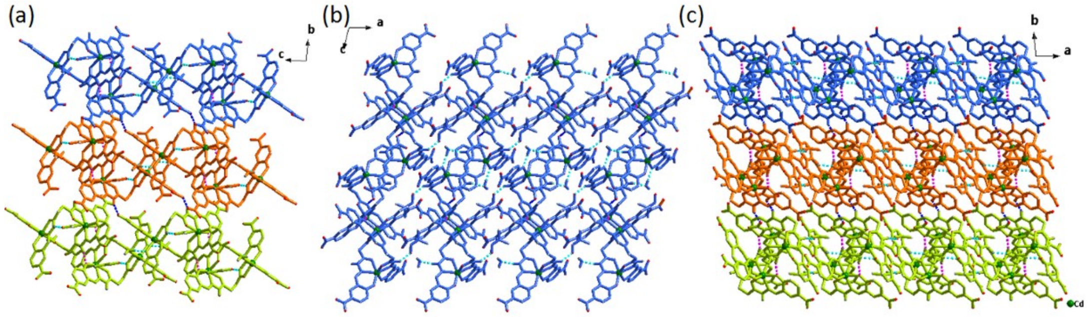

Fig. S5 3D supramolecular structure of Cd-L from a, b, c axis. The H-bonding linking between binuclear structures: dashed lines.

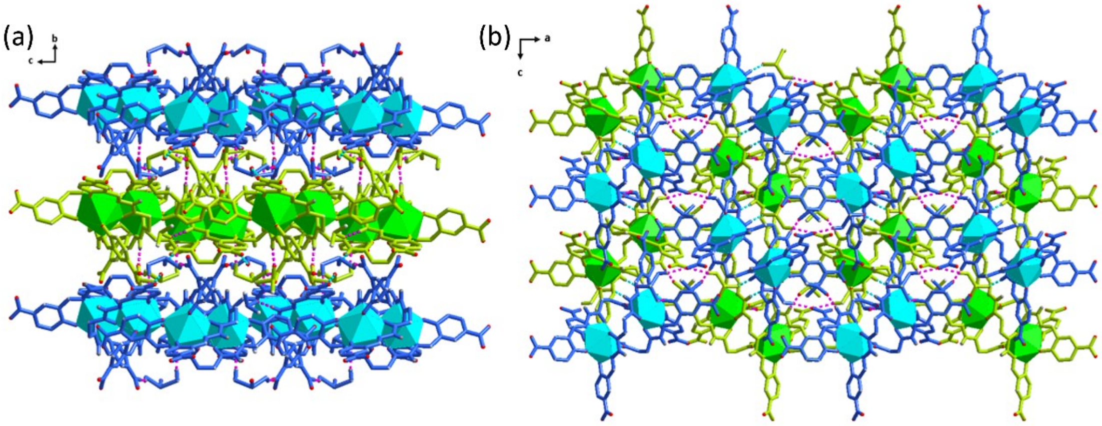

Fig. S6 3D supramolecular structure of **Eu-L** from a axis (a) and b axis (b). The H-bonding linking between binuclear structures: dashed lines.

Thermal stability

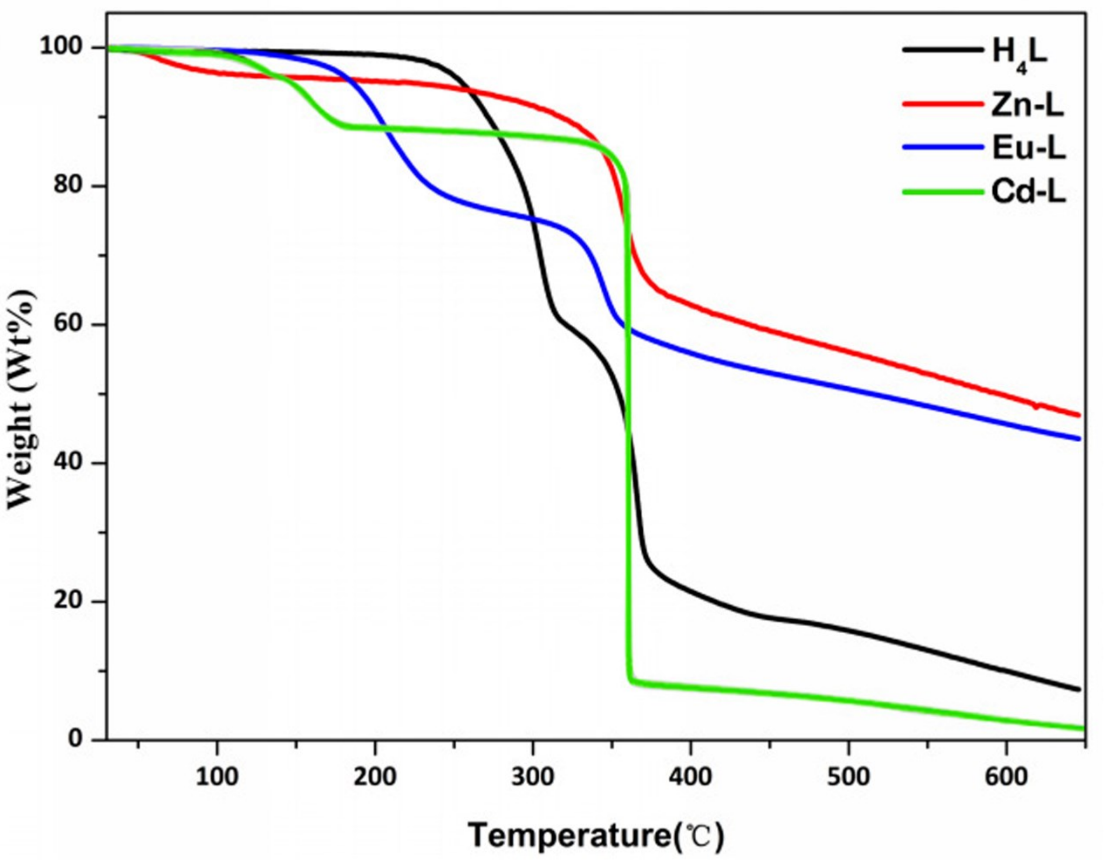

Fig. S7 TG analysis curves of **H_4L** and complexes **Zn-L**, **Cd-L**, **Eu-L**.

TGA was employed for **H_4L**, **Zn-L**, **Cd-L** and **Eu-L** to probe their thermal stability. When the temperature of the ligand **H_4L** came up to 250 °C, two acylhydrazone bonds were successively broken, accompanied by the mass loss accounted for 38.27% and 37.41% of the total mass(Cal. value 40.53%), respectively. The mass loss of the complex **Zn-L** was 27.46% of the total mass, corresponding to the loss of five DMF molecules (Cal. value 26.47%). The mass loss of the complex **Cd-L** at 130 °C was 11.34% of the total mass, corresponding to the loss of DMF molecule and H_2O molecule (Cal. value 10.81%). As for complex **Eu-L**, the mass loss at 160 °C was 22.02% of the total mass, corresponding to the loss of six DMSO molecules (Cal. value 22.66%). For the three complexes, they begin to collapse when the temperature rises to ***ca.*** 350 °C, which indicated that they have good thermal stability.

General spectroscopic methods

Solution fluorescence titration spectra and selectivity experiments were checked using a PERSEE TU-1950 luminescence spectrometer. Stock solutions (3 × 10^{-2} M) of the salt solutions of metal ions $LiCF_3SO_3$, $NaCF_3SO_3$, $(CF_3SO_3)_2Mg$, $(CF_3SO_3)_3Al$, KCF_3SO_3, $(CF_3SO_3)_2Ca$, $CrCl_3$, $MnCl_2$, $FeCl_3$, $CoCl_2$, $NiCl_2$, $CuCl_2$, $ZnCl_2$, $CdCl_2$ were prepared. High concentrations of the stock solution **H_4L**(1.0 mM) were prepared in DMF solution. Before spectroscopic measurements, the solution was freshly prepared by diluting the high concentration stock solution to the corresponding solution.

Optical properties

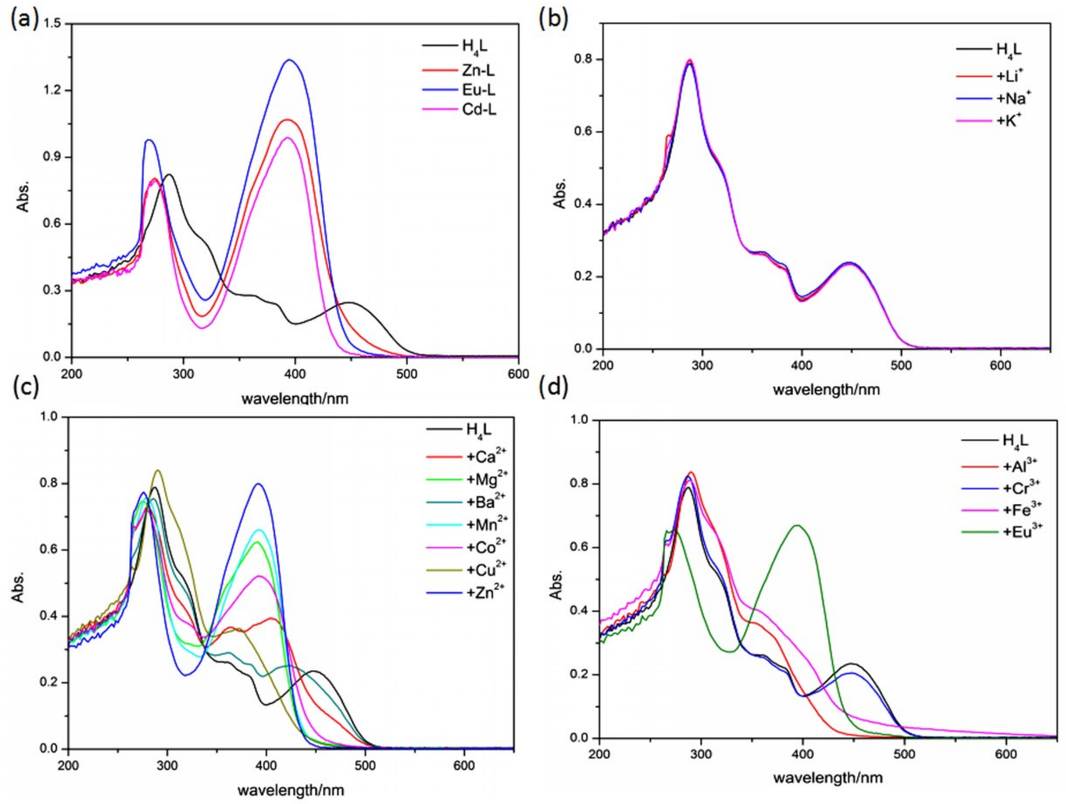

Fig. S8 UV-vis absorption spectra of **H_4L**, **Zn-L**, **Cd-L**, **Eu-L** in 2.0 × 10^{-5} M DMF(a), UV-vis absorption after adding 1 equiv. of monovalent(b), divalent(c), and trivalent(d) metal ions to **H_4L** solution (2 × 10^{-5} M, DMF).

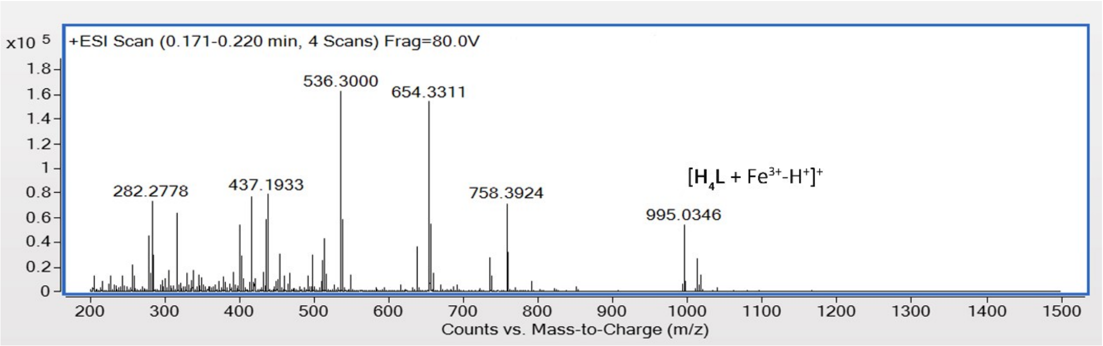

Fig. S9 The mass spectra of the complex between H_4L and Fe^{3+}.

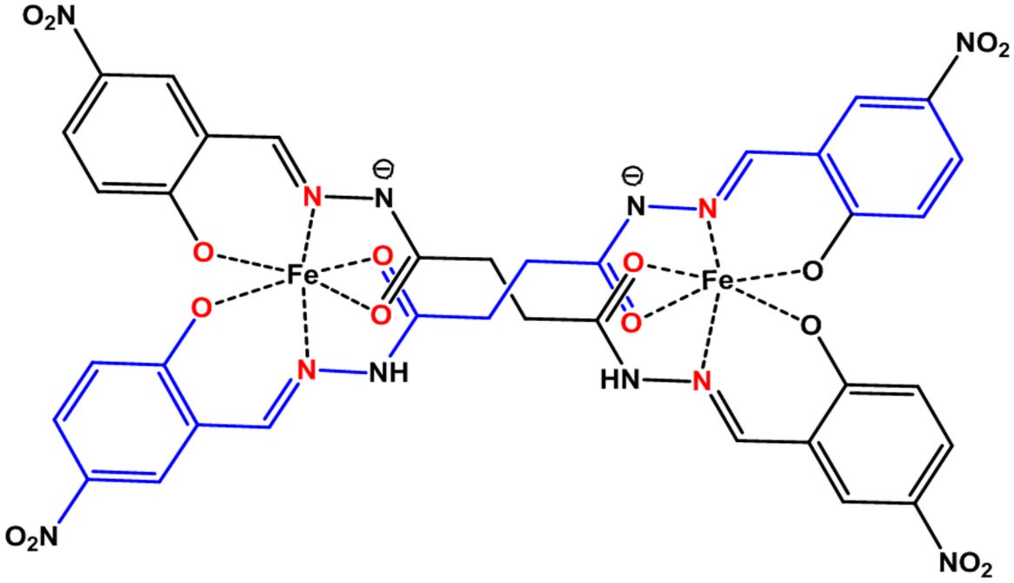

Fig.S10 The possible combination mode between ligand H_4L and Fe^{3+} ions.

Based on the detection by IUPAC (CDL = 3σ/k), the detection limit of **H_4L** for Fe^{3+} was estimated to be 4.2×10^{-5}mol/L. Although the detection limit is not too low, this study provides a reliable basis for the identification of Fe^{3+} by Schiff base of diacylhydrazone in the future.

Table S5 The fluorescence intensities of 10 blank solutions at 417nm

No.	1	2	3	4	5	6	7	8	9	10
Int.	3190	3182	3187	3181	3107	3126	3020	3074	3100	3229

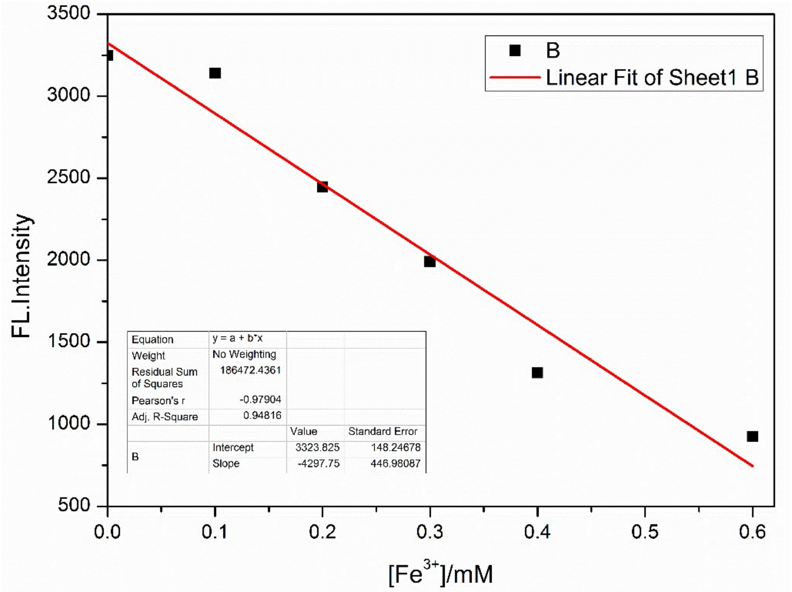

Fig. S11 The calibration curve of fluorescence intensities at 417nm.